Journal of Applied Research and Technology

www.jart.ccadet.unam.mx
Journal of Applied Research and Technology 16 (2018) 455-465

Original

Tungsten based catalysts for oxidative desulfurization: surface species and partially reduced systems as key features to improve the activity

Mauricio Lopez Luna*, Luis Cedeño-Caero

Departamento de Ingeniería Química, Facultad de Química, Universidad Nacional Autónoma de México, Ciudad de México 04510, México

Abstract: Tungsten oxide based catalysts for the oxidative desulfurization (ODS) process of dibenzothiophene compounds using H_2O_2 as oxidizing agent were studied. Catalysts were characterized by TPR-H_2, SEM-EDS, XRD, N_2-physisorption and Raman spectroscopy. Different surface tungsten oxide species were detected and related to the ODS activity, furthermore, the predominance of the surface tungsten oxide species was associated with the tungsten loading. Moreover, in some catalysts, WO_3 crystals were detected and their role in the performance of the catalysts was studied too. Finally, the catalysts were partially reduced and tested in the ODS reaction, the reduced catalysts exhibited high activity and an improvement of H_2O_2 to sulfones yield.

Keywords: ODS; Tungsten oxide; TPR-H_2; Alumina; Low sulfur diesel; Dibenzothiophene compounds

1. INTRODUCTION

Sulfur regulations around the world have established ultra-low sulfur contents for fuels. The sulfur content in diesel allowed in Mexico, Europe and the USA is less than 10 ppm (NOM 086 2005, 2008; International Energy Outlook 2016). In order to attend the regulations, the conventional process of fuel desulfurization, the hydrodesulfurization (HDS), has suffered some modifications to reach the ultra-low sulfur diesel contents (ULSD) established by the environmental policies (International Energy Outlook 2016; Mjalli, Ahmed, Al-Wahaibi, Al-Wahaibi, & AlNashef, 2014; NOM 086 2005, 2008; OPEC, 2011; World Energy). Among the main adjustments stand out H_2S removing from the reactor, increasing the LSHV, increasing the reactor dimension, using multistage HDS systems and using more active catalysts. Nevertheless, all of these solutions are expensive (Speight & El-Gendy, 2015).

Another recent alternative to achieve the ULSD is to interconnect the HDS process with a complementary process. The additional process must be specialized in removing the refractory compounds of the HDS process (Song, 2003). One of the most promising processes for

* Corresponding author.
E-mail address: mauricio.lopez.luna.chem.eng@gmail.com (M. Lopez Luna).

Peer Review under the responsibility of Universidad Nacional Autónoma de México.

http://

interconnecting with conventional HDS process is the oxidative desulfurization process (ODS), which is able to remove refractory dibenzothiophene compounds (DBTs) such as dibenzothiophene, 4-methyl dibenzothiophene and 4,6-dimethyl dibenzothiophene (Mjalli, 2014).

The ODS process consists of the oxidation of DBTs to sulfones using oxidating agents. The sulfones generated during the oxidation are easily extracted from the fuel phase using physical methods, commonly a liquid extraction with acetonitrile (Murata, Murata, Kidena, & Nomura, 2004; Otsuki et al., 2000; Stanislaus, Marafi, & Rana, 2010; Te, Fairbridge, & Ring, 2001). In this context, an HDS conventional process interfaced to an ODS process could achieve ULSD.

In order to reach a commercially attractive ODS technology, two issues have to be addressed to reduce the ODS process limitations: more active and cheaper catalysts should be developed and the extraction of sulfones should be improved. In recent years, the research in ODS catalysts has been focused on the development of new metal and bimetallic-based catalysts supported on cheap high surface metal oxides (Feng, 2010; Qian, 2008; Li, Zhu, Wang, Wang, & Chen, 2012). The interactions and synergy found in bimetallic based catalysts are still under discussion. The relationship and phenomena caused by the interaction of multiple metals oxides on the ODS performance have not been clearly established (Bakar, Ali, Kadir, & Mokhtar, 2012; Gónzalez-García & Cedeño-Caero, 2010; Mokhtar, Bakar, Ali, & Kadir, 2016).

Many studies using metal oxides such as V, Cr and Mo (Ismagilov et al., 2011; Qian, 2008; Stanislaus et al., 2010) have shown good performance for ODS. However, vanadium and molybdenum based catalysts tend to be leached into the liquid phase during the reaction and chromium based catalysts are less active than molybdenum and vanadium based catalysts (Alvarez-Amparan, & Cedeño-Caero, Cortes-Jácome, & Toledo-Antonio, 2017; Cedeño-Caero & Alvarez-Amparan 2014; Cedeño-Caero, Gomez-Bernal, Fraustro-Cuevas, Guerra-Gomez, & Cuevas-Garcia, 2008; González-Garcia & Cedeño-Caero, 2009). Thus, in order to develop more stable and active catalysts, tungsten oxide based catalysts have received more attention, especially due to the strong interaction between some supports (such as alumina) (Arena, Frusteri, & Parmaliana, 1999; Wachs, Chersich, & Iiardenbergh, 1985) and tungsten oxide. Furthermore, it has been reported that tungsten oxide based catalysts exhibit a good performance for oxidizing processes (Bakar, 2012; Feng, 2010).

Herein, tungsten based catalysts are studied as catalysts for ODS. Mostly, the study of the surface species formed by the interaction between the alumina support and the metal oxide is addressed by TPR-H_2, Raman spectroscopy, XRD, SEM-EDS and N_2-physisorption characterizations. Moreover, the catalytic performance of some partially reduced tungsten based catalysts is discussed.

2. EXPERIMENTAL

2.1 CATALYST PREPARATION AND CHARACTERIZATION

All catalysts were prepared by incipient impregnation method using -alumina (213 m^2/g) as support. The catalysts were prepared using a water solution of ammonium metatungstate hydrate (Sigma-Aldrich, 89 %). After the impregnation step, the samples were dry at 120 °C for 12 h and then calcined by 5 h at 500 °C in a quartz reactor with a continuous feed of dry air (15 mL/min). The catalysts were labelled according to their tungsten loading as Wx, where x indicates the metal loading (% wt). Some calcined catalysts were reduced up to 750 °C in TPR-H_2 equipment and the letter "R" was added to the label, i.e. W17R corresponding to the catalyst with 17 wt.% of W and reduced at 750 °C.

In order to characterize the surface oxide species, TPR-H_2 studies were carried out, the TPR-H_2 experiments were performed in a conventional temperature programmed reduction apparatus. The test was carried out using a flow of an H_2/Ar mixture (70% H_2, 25 cm^3/min) with a heating rate of 10 °C/min up to1000 °C, if necessary, the sample was kept at this temperature until the reduction was completed. In the case of the partially reduced catalysts, the reduction was carried out up to 750 °C using the same flow and heating rate.

Elemental composition was evaluated by SEM-EDS using a Jeol JSM-5900 LV microscope equipped with an energy dispersive X-ray elemental analysis system (EDS) Oxford-ISIS. Textural properties were measured by N_2 adsorption-desorption isotherms of the samples at 77 K using a Tristar Micrometrics apparatus. The isotherms were analyzed by the BJH method. Before each textural analysis, the samples were degassed for 8 h in vacuum at 350°C. XRD studies were carried out with a Siemens D500

powder diffractometer with Cu K radiation from 20 to 70 degree in two theta scale with a step size of 0.02 s. Raman spectroscopy was used to obtain further information of the tungsten oxide surface species, the Raman spectra were recorded from a stationary sample at room temperature and pressure. The samples were analyzed with a DxR Raman microscope Thermo Scientific using a 532 nm line as the excitation source and the spectral resolution was 1 cm^{-1}. The acquisition time for each spectrum was 20 s and 50 scans were averaged.

2.2 CATALYTIC EXPERIMENTS

Activity tests were carried out in a glass batch reactor jacketed in a thermally controlled water bath at 60 °C and atmospheric pressure fitted with a condenser and mechanical stirrer. A model mixture with a total S content of 609 ppm was prepared using acetonitrile (Empura, 99%) as solvent and S-compounds (DBTs): dibenzothiophene (DBT, Sigma-Aldrich, 98%), 4-methyl dibenzothiophene (4-MDBT, Sigma-Aldrich, 96%) and 4,6-dimethyl dibenzothiophene (4,6-DMDBT, Sigma-Aldrich, 97%). In a typical run, 50 cm^3 of the model mixture, catalyst (100 mg) and 0.5 mL of H_2O_2 (PQF, 30%, V/V) were added to the reactor with vigorous stirring (750 rpm) for avoiding mass transfer issues (Cedeño-Caero et al., 2008; González-García & Cedeño-Caero, 2009; 2010). The initial molar ratio of the oxidizing agent/sulfur compound (O/S) was 6. If the O/S ratio decreased below 2, small amounts of H_2O_2 were added for maintaining the O/S ratio around 6. Reaction products were analyzed by gas chromatography, the analysis was performed in an HP5890 Series II Gas Chromatograph with a PONA capillary column (Methyl silicone Gum, 50 m x 0.2 mm x 0.5 m film thickness). Reactant and product identifications were achieved with GC-PFPD (Varian CP-3800) and GC-MS (HP5890 Series II with MS detector). H_2O_2 concentration was measured by standard iodometric titration.

3. RESULTS

3.1 TUNGSTEN OXIDE BASED CATALYSTS

In order to measure the intrinsic catalytic activity of the catalysts, ODS tests were carried out in a simplified 2 phases ODS system (extraction solvent and solid catalyst), considering extraction step of sulfur compounds from hydrocarbon phase is faster than oxidation step (Bernal & Caero 2005; Ismagilov et al., 2011). The Fig. 1 shows the DBT-sulfone yield in function of time, for simplicity, only DBT-sulfone yield is shown since all the other DBTs show similar tendencies.

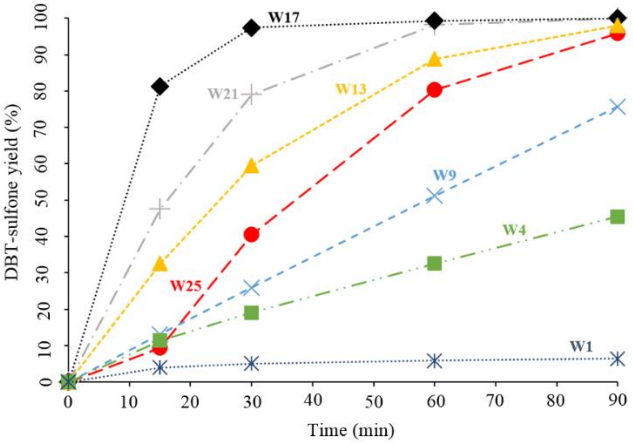

Fig. 1. Catalytic performance for DBT oxidation of tungsten based catalysts.

The catalytic performance of the tungsten oxide catalysts is highly dependent on the metal loading in each catalyst. Low loading catalysts such as W1, W4 and W9 (1, 4, and 9 % wt tungsten loading) exhibit low yield throughout the catalytic tests. W13 and W17 exhibit a better performance than the catalysts with lower loading, reaching around the 100% of the DBT-sulfone yield throughout the reaction time. However, the catalysts with a higher tungsten loading (W21 and W25) show a decrease in the catalytic performance in comparison with W17.

In general, the results showed in Fig. 1. fit very well with a first-order reaction comportment, in consequence, the kinetic constants associated with these catalysts were calculated using a first-order fit and are shown in Table 1, moreover, the molar percentage of H_2O_2 that reacted to form sulfones (H_2O_2 to sulfones yield) is shown. Additionally, the kinetic constants of DBTs oxidation are plotted in Fig.2 in function of the surface density of tungsten, considering a homogeneous distribution of the metal loading on the support.

The value of the kinetic constants increases with the tungsten metal loading until 2.68 atoms/nm^2, then, there is a decrease of the kinetic constants with the increase in metal loading. Furthermore, the activity increase is more remarkable at around 2 and 2.7 atoms/nm^2, while the increase in activity between 0 and 2 atoms/nm^2 is less representative. This behaviour is observed for all the DBTs tested. It is important to point out that the increase

in the kinetic constant value, between 0 and 2.68 atoms/nm^2, is nonlinear with the metal loading increase, suggesting that the increase in activity is not only related to an increase in active phase in the catalysts.

The XRD patterns of the tungsten oxide based catalysts are shown in Fig. 3. In general, there are not crystalline phase with the exception of W25 and W21 which present small diffraction peaks at 23, 24, 33 and 34 degrees. According to the references, these diffraction peaks are assigned to WO_3 (monoclinic) (Kuzmin, Purans, Cazzanelli, Vinegoni, & Mariotto, 1998).

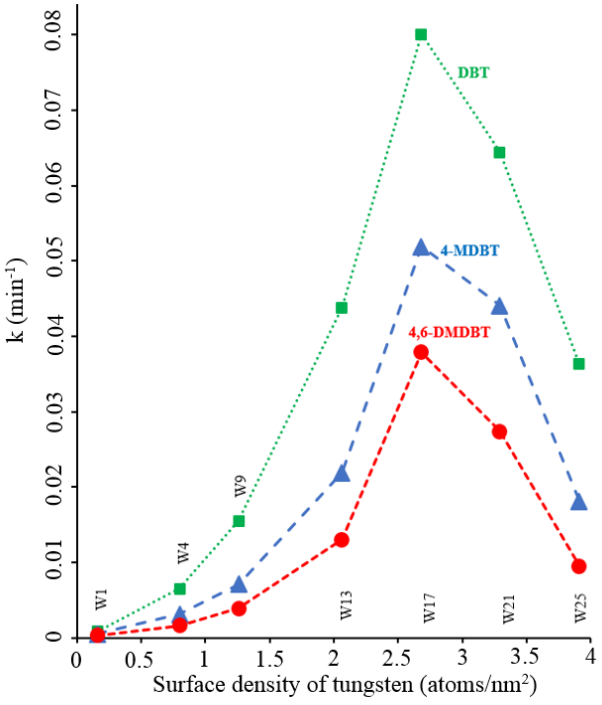

Fig. 2. Pseudo-first order kinetic constants of DBTs oxidation in function of surface density of tungsten.

The SEM-EDS and N_2-physisorption analysis of the tungsten oxide based catalysts are shown in Table 2. In general, the theoretical loading matches with the experimental composition detected. Moreover, the SEM images (not shown) do not show agglomerates of oxide metal except for W25 and W21, this result supports the results obtained from XRD. Regarding the textural properties, the surface area and pore volume decrease with the increase in metal loading, this trend has been observed and discussed in previous works (Loefanti et al., 1997; Massoth, 1979; Mitra, Wachs, & Deo, 2006; Schneider, Hudec, & Solcova, 2008) and it is related to porosity obstruction by the increase in metal oxide loading.

TPR-H_2 profiles obtained from the tungsten oxide based catalysts are shown in Fig. 4, moreover, the reduction profile of bulk WO_3 is shown as a reference. Bulk WO_3 reduction profile exhibits two main peaks with a temperature of reduction rate maximum (T_{max}) at 605 and 730 °C, furthermore, there are two shoulders, one before the first peak and the second before the second peak. WO_3 reduction takes place in three steps (Ogata, Kamiya, & Ohta, 1973), the first step corresponds to reduction WO_3 to $W_{20}O_{58}$ and it is associated with the shoulder between 490 and 550 °C. The second step is the $W_{20}O_{58}$ reduction to WO_2 and corresponds with the reduction peak with T_{max} at 605 °C. Finally, the third step is the WO_2 reduction to W and is associated with the reduction peak with T_{max} at 730 °C. The shoulder after the peak at 730 °C is associated with diffusional issues in the third reduction step (Magnus, Bos, & Moulijn, 1994; Vermaire & Van Berge, 1989).

W1 reduction profile does not show any reduction peak, this could be due to the low tungsten loading (0.15 atoms/nm^2) that leads to form very strong interactions with alumina, which cannot be reduced at temperatures of 1000 °C. W4 shows a reduction profile with a dominant peak between 870 and more than 1000 °C with the T_{max} above the 1000 °C, W9 exhibits a peak like the peak of W4, but the T_{max} is at 976 °C. W13 exhibits a peak with a T_{max} of around 940 °C and W17 exhibits a broader peak with a T_{max} at 877 °C. In W4, W9, W13 and W17, as the metal loading increases, the reduction begins at lower temperatures and the peak is broader.

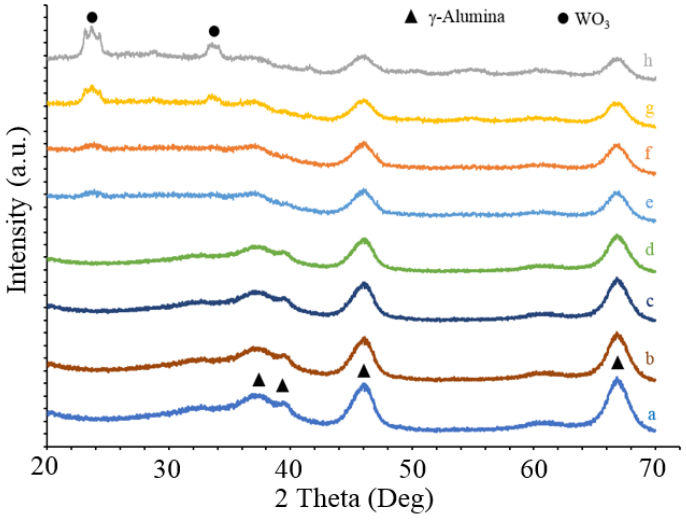

Fig. 3. XRD patters of (a) γ-alumina, (b) W1, (c) W4, (d) W9, (e) W13, (f) W17, (g) W21 and (h) W25.

Table 1. Pseudo-first order kinetic constants of DBTs oxidation to sulfones and H_2O_2 to sulfones yield for tungsten based catalysts.

Catalyst	Kinetic constant (min^{-1})			Total H_2O_2 consumption (mmol)[a]	H_2O_2 to sulfones yield (%)[a]
	k_{DBT}	$k_{4\text{-MDBT}}$	$k_{4,6\text{-DMDBT}}$		
W1	0.0008	0.0005	0.0003	0.4	45.8
W4	0.0065	0.0031	0.0016	1.1	38.4
W9	0.0155	0.0071	0.0039	1.9	42.2
W13	0.0438	0.0219	0.0130	2.6	46.9
W17	0.0801	0.0519	0.0379	2.7	53.4
W21	0.0644	0.0441	0.0274	2.8	49.3
W25	0.0363	0.0181	0.0095	3.1	36.1

[a] Calculated at 90 min of reaction.

Table 2. Metal loading and textural properties of tungsten based catalysts.

Catalyst	W (%) theoretical	W (%) experimental	W (atoms/nm²) theoretical	W (atoms/nm²) experimental	Surface area (m^2/g)	Pore volume (cm^3/g)
W1	1	1.3	0.15	0.20	211	0.37
W4	4	3.9	0.63	0.62	205	0.33
W9	9	8.6	1.42	1.36	197	0.31
W13	13	14.1	2.06	2.24	184	0.31
W17	17	17.3	2.68	2.73	173	0.3
W21	21	20.4	3.29	3.20	157	0.27
W25	25	27.9	3.91	4.37	141	0.23

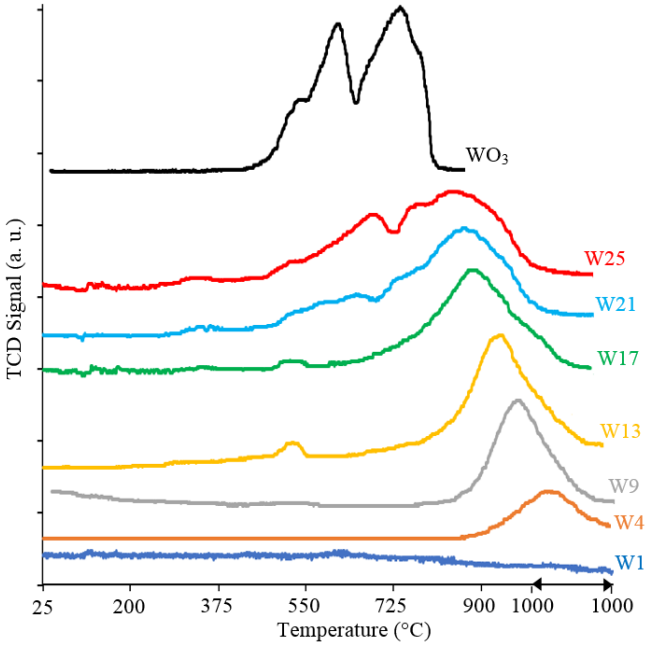

Fig. 4. TPR-H_2 profiles of tungsten based catalysts and bulk WO_3.

The peak observed in W4, W9, W13 and W17 profiles is associated with the reduction of WO_4 tetrahedral surface species and WO_6 octahedral surface species (Fierro, 2006; Salvati, Makovsky, Stencel, Brown, & Hercules, 1981). WO_6 species are polymerized in continuous two-dimensional chains, their formation is enhanced at high tungsten oxide loadings and began to reduce between 620 °C and more than 900 °C (Horsley, Wachs, Brown, Via, & Hardcastle, 1987; Thomas, De Beer, & Moulijn, 1981). The WO_6 species are reduced in a large temperature range due to different degrees of polymerization which imply different resistances to be reduced. WO_4 species are isolated or as a dimer (Vuurman & Wachs, 1992; Vuurman, Stufkens, Oskam, Deo, & Wachs, 1996; Weckhuysen, Jehng, & Wachs, 2000) and they are reduced at temperatures up 900°C, in fact, the catalyst W4 points out a T_{max} above the 1000 °C.

W21 and W25 show reduction profiles with the same main peak than W4, W9, W13 and W17. Moreover, there

are several shoulders between 550 and 750 °C, like WO_3 reduction profile, suggesting that exist tungsten oxide crystals in these catalysts in addition to the single surface species discussed for the catalysts W4, W9, W13 and W17. Finally, the small peak around 520 °C observed in W13, W17, W21 and W25 corresponds with a small formation of microcrystals or clusters of WO_3 (Reddy & Varma, 2004; Thomas et a.,1981; Vermaire & Van Berge, 1989), and there are formed due to small cationic impurities on the alumina (Vurrman et al.,1996).

Raman spectra of W25, W21, W17 and W13 are shown in Fig. 5. W13 exhibits a spectrum with a strong Raman band at 963 cm^{-1}, moreover, there is a band centred at 880 cm^{-1} and a pair of weak bands at 352 and 219 cm^{-1}. The Raman band at 963 cm^{-1} is assigned to the symmetric stretch of W=O bond. For hydrated conditions, the Raman band associated with the symmetric stretch of W=O changes according to the predominance of WO_4 (951 cm^{-1}) or WO_6 species (975 cm^{-1}) (Kim, Burrows, Kiely, & Wachs, 2007; Ostromecki, Burcham & Wachs 1998; Wachs & Roberts, 2010). Therefore, the band at 963 cm^{-1} for W13 is generated by a combination of WO_4 and WO_6 species. The Raman band at 880 cm^{-1} is assigned to the symmetric stretch of O-W-O bonds from WO_6 polymerized species (Ostromecki, Burcham, Wachs, Ramani, & Ekerdt, 1998; Vuurman & Wachs, 1992). The band at 352 cm^{-1} is related to bending mode of WO_6 and WO_4 species (Ostromecki et al., 1998), it shifts its position according to the WO_6/WO_4 ratio change, taking lower values when to WO_6/WO_4 ratio increases. The band at 219 cm^{-1} is associated with the bending mode of polymeric W-O-W linkages (Horsley et al., 1987; Vuurman & Wachs, 1992).

W17 possesses the same bands that W13, however, the main band in W17 is centred at a higher value (968 cm^{-1}) and the band at 352 cm^{-1} in W13 is shifted to 338 cm^{-1} in W17. According to the references, the shift of these bands is related to a change in the WO_6/WO_4 ratio, the shift in these bands is associated with an increase in WO_6 species. Moreover, the peak associated with the W=O symmetric stretch in W9, W4 and W1 (not shown) tend to 951 cm^{-1} indicating a higher presence of WO_4 species while the tungsten loading decrease.

Regarding W21 and W25, the Raman bands at 806, 714 and 270 cm^{-1} are associated with WO_3 crystalline phase (Daniel, Desbat, Lassegues, Gerand, & Figlarz, 1987). Moreover, W21 shows a weak Raman band at 977 cm^{-1} indicating WO_6 species, this result points out that W21 (3.29 atoms/nm^2) possesses tungsten surface species and tungsten crystalline phase at the same time which could be an indicator of this catalyst is just above the monolayer coverage.

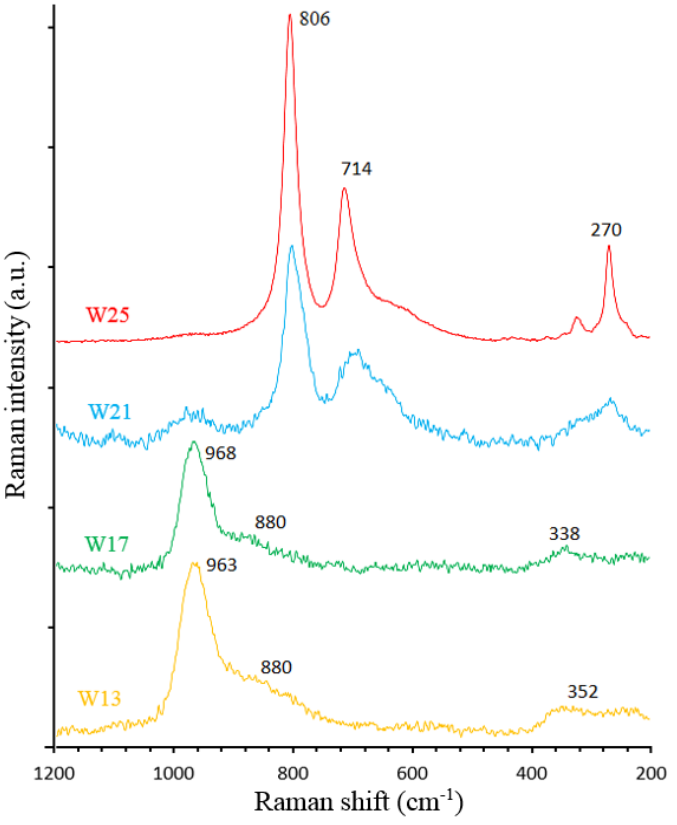

Fig. 5. Raman spectra of high loading tungsten oxide based catalysts.

3.2 PARTIALLY REDUCED TUNGSTEN BASED CATALYSTS

Some tungsten oxide based catalysts were partially reduced at 750 °C in a continuous H_2 flow. The results of the catalytic tests of reduced catalysts are shown in table 3, the letter "R" was added to the label to indicate that the catalysts were partially reduced up to 750 °C.

All reduced catalysts show a high kinetic constant value and possess a high H_2O_2 to sulfones yield. Moreover, the W loading in the reduced catalyst does not affect significantly the value of the kinetic constants. Results in SEM micrographs and N_2-physisorption (not shown) displayed the formation of metal particles over the surface and specific surface areas around 125 m^2/g for all reduced catalysts. These results suggest a loss of area due to a

collapse of micropores in the support during the high-temperature reduction and a decrease of the dispersion of the active phase owing to the formation of clusters and metal particles.

4. DISCUSSION

4.1 TUNGSTEN OXIDE SURFACE SPECIES AND ODS ACTIVITY

Below the monolayer coverage, the tungsten oxide catalysts showed a nonlinear increase in their activity whit the increase in the tungsten loading. There is a considerable increase in activity around the catalysts W13 (2.06 atoms/nm^2), which is 3-fold more active than W9 and only possesses around 50% more active phase. This same phenomenon can be observed between the catalysts W17 and W13 showing that W17 is 2-fold more active than W13 but W17 only possesses around a 30% more active phase than W13. Supporting the previous, the catalyst W9 is around the double of active than W4, which corresponds with a linear relationship between the tungsten loading and the increase in activity. These differences point out that the activity does not increase just for the increase in the tungsten loading. Furthermore, the activity decreases for W21 and W25, according to the characterizations, this is due to the loading is above the monolayer coverage and WO_3 crystalline phase has been formed on the surface blocking the active sites.

According to the results in TPR-H_2, there is a change in the type and predominance of tungsten surface species over the alumina surface, which coincide with the change in activity observed in the catalytic tests. The TPR-H_2 results pointed out that at low tungsten loadings, species WO_4 is formed over the surface, and when the tungsten loading increases, there is a change in the peak of reduction associated with the formation of WO_6 species, especially after the 2.06 atoms /nm^2 (W13). Moreover, the whole reduction peak is shifted to lower temperatures pointing out the presence of several WO_6 polymerized chains. At the same time, the peak associated with WO_4 becomes less representative with the loading increase.

Regarding Raman spectroscopy, the same change in the predominance of surface species (WO_4 and WO_6) is observed. High tungsten loading enhances the formation of WO_6, while the WO_4 species becomes fewer commons. This could be due to the WO_4 species are forced to polymerize with other WO_4 species to form WO_6 due to a decrease in the number of hydroxyl groups available over the alumina surface. Small tungsten loadings allow the formation of WO_4 species which have a stronger interaction with the alumina than WO_6. However, with the increase in tungsten loading and due to the strong interaction between the alumina and the tungsten oxide, the WO_4 species could be forced to change their coordination and polymerized between them to allow more tungsten oxide surface species over the alumina.

In order to explain how the surface tungsten oxide species are related to the activity of the catalysts, it is necessary to consider previous studies related to the ODS mechanism (Bregeault, 2003; Campos-Martin, Capel-Sanchez, Perez-Presas, & Fierro, 2010; García-Gutiérrez et al., 2008; Ishihara et al., 2005; Rafiee, Sahraei, & Moradi, 2016; Rezvani, Oveisi, & Asli, 2015). The ODS reaction mechanism in aprotic solvents, as acetonitrile, using H_2O_2 as oxidizing agent, occurs by a nucleophilic attack of the sulfur compound to peroxo complex formed by the metal oxide surface species and the H_2O_2 molecule. The Fig. 6 shows the possible mechanism for the oxidation of DBTs by WO_6 surface species.

The mechanism consists in three steps: (1) the formation of a hydroperoxytungstate by a nucleophilic attack of the H_2O_2 to the surface species, (2) a peroxo complex is formed by the loss a water molecule and (3) the sulfur molecule makes a nucleophilic attack on the peroxo complex to form a sulfoxide and then, by a similar way, to form the sulfone.

The high degree of coordination of WO_6 in comparison with WO_4 species suggests that WO_6 polymerized species are more susceptible to nucleophilic attacks. In WO_6, the electronegativity of the 6 oxygen atoms generates a high coordinated tungsten atom susceptible to nucleophilic attacks. The formation of the hydroperoxytungstate and the oxidation of the sulfur compound by the peroxo complex occurs by nucleophilic attacks, therefore, the surface species with metal cores with lack of electrons favour the steps 1 and 3 of the mechanism, showing a higher activity in the oxidation of DBTs.

Regarding the catalysts W21 and W25, the decrease in activity can be explained by the results of XRD, TPR-H_2 and Raman spectroscopy. All of these characterizations showed evidence of crystalline phase over W21 and W25. Possibly, the crystalline phase blocks the surface tungsten oxide species, and at the same time, it points out that the crystalline phase is less active than the surface tungsten

Table 3. Pseudo-first order kinetic constants of DBT oxidation to sulfones and H_2O_2 to sulfones yield for the reduced catalysts.

Catalyst	Kinetic constant (min^{-1})			Total H_2O_2 consumption[a] (mmol)	H_2O_2 to sulfones yield (%)[a]
	k_{DBT}	$k_{4\text{-MDBT}}$	$k_{4,6\text{-DMDBT}}$		
W13R	0.0757	0.0521	0.0319	1.9	72.9
W17R	0.0786	0.0522	0.0302	2.2	64.0
W21R	0.0801	0.0571	0.0335	2.2	63.0
W25R	0.0805	0.0527	0.0329	2.1	65.9

[a] Calculated at 90 min of reaction.

oxide species. Moreover, the results of H_2O_2 consumption (Table 1) of W21 and W25 indicate that there is an increase in H_2O_2 consumption but a decrease in the sulfones production, this result suggests that the WO_3 crystalline phase promotes the decomposition of H_2O_2 instead of to use it to produce sulfones.

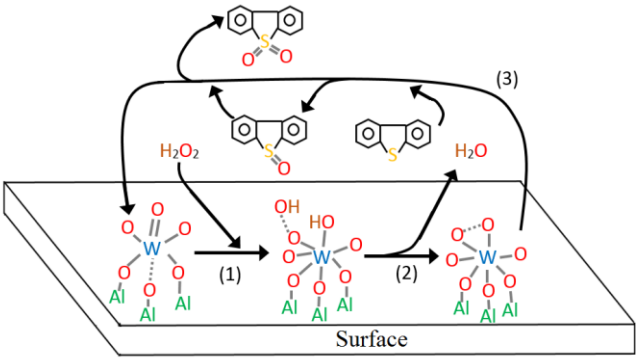

Fig. 6. A possible mechanism for the oxidation of DBT by H_2O_2-WO_6 surface species.

4.2 PARTIALLY REDUCED CATALYSTS AND ODS ACTIVITY

According to the activity tests of partially reduced catalysts, there is a remarkable change in their behaviour in comparison with the calcined tungsten based catalysts. All of the reduced catalysts showed high activity, and a better H_2O_2 to sulfones yield than the calcined catalysts (Table 1 and Table 3) without considering the tungsten loading. Moreover, during the catalytic test, all partially reduced catalysts showed poor activity the first 15 min of reaction (not shown), but then, the activity increased considerably. This phenomenon could be associated with a "kinetic delay period", which could be related to a reoxidation of the tungsten species over the catalysts which take the role of the active phase.

These results point out a new way to catalyze the ODS reaction, the partially reduced catalysts possess different active phases and exhibit activities and selectivities (H_2O_2 to sulfones yield) comparable to the best tungsten oxide based catalyst (W17). These results are similar to a previous work where a system based on Mo-V was studied (Alvarez-Amparan & Cedeño-Caero, 2017; González-García & Cedeño-Caero, 2010; 2009), in such study, an increase in ODS activity was reported when the catalysts were partially reduced, regardless the loss of surface area and the metal loading. These results suggest that the partially reduced catalysts possess a high activity and overall DBTs yield. Nevertheless, an exhaustive study is needed for understanding completely the performance of partially reduced tungsten based catalysts.

5. CONCLUSIONS

Tungsten oxide based catalysts were prepared characterized and tested in ODS reaction. The calcined catalysts showed WO_6 and WO_4 surfaces species on the alumina surface. The predominance of each species was set by the tungsten loading. Catalysts with a high quantity of WO_6 species exhibited better ODS activities than the catalysts with WO_4 species and few WO_6 species. The catalysts with a high amount of WO_6 species resulted in more active catalysts and such activity improvement could be attributed to high coordination of the WO_6 species that makes the metal core more vulnerable to nucleophilic attacks. Therefore, the WO_6 species are the principal contribution to the activity in the DBTs oxidation by H_2O_2 and represent a promising design parameter to develop a more active catalyst for ODS. On the other hand, the WO_3 crystalline phase blocks the surfaces species and leads to a decrease in activity, moreover, the WO_3 causes a decrease in the H_2O_2 to sulfones yield indicating that the crystalline phase promotes the H_2O_2 decomposition. Therefore, the formation of the crystalline phase must be avoided during the synthesis of the catalysts in order to achieve better performances.

The partially reduced catalysts showed ODS activities comparable to the best tungsten oxide based catalyst and they show similar activities among them regardless of the metal loading. Moreover, the partially reduced catalysts showed an improvement in the selectivity (H_2O_2 to sulfones yield: around 10%) pointing out them as a promising system to develop better ODS catalysts. The new catalytic species involved in the partially reduced catalysts could be formed by the influence of the H_2O_2 which could re-oxidate the partially reduced tungsten species, however, the question of what are the catalytic species and what is the catalytic mechanism remains, further research is required in order to shed light on this system.

ACKNOWLEDGEMENTS

This work was supported by the Project Support Program for Research and Technological Innovation (PAPIIT) of UNAM (Project IN-115317). Mauricio Lopez Luna acknowledges the national scholarship (scholarship number: 417869) to The Mexican National Council for Science and Technology (CONACyT). We thank M. Cristina Zorrilla Cangas for the technical assistance (Raman spectroscopy).

CONFLICT OF INTEREST

The authors have no conflicts of interest to declare.

REFERENCES

Alvarez-Amparán, M. A., & Cedeño-Caero, L. (2017). MoOx-VOx based catalysts for the oxidative desulfurization of refractory compounds: Influence of MoOx-VOx interaction on the catalytic performance. Catalysis Today, 282, 133-139.

Alvarez-Amparán, M. A., Cedeño-Caero, L., Cortes-Jácome, M. A., & Toledo-Antonio, J. A. (2017). Relationship between the catalytic activity and Mo–V surface species in bimetallic catalysts for the oxidative desulfurization of dibenzothiophenic compounds. Reaction Kinetics, Mechanisms and Catalysis, 122(2), 869-885.

Arena, F., Frusteri, F., & Parmaliana, A. (1999). Structure and dispersion of supported-vanadia catalysts. Influence of the oxide carrier. Applied Catalysis A: General, 176(2), 189-199.

Bakar, W. A. W. A., Ali, R., Kadir, A. A. A., & Mokhtar, W. N. A. W. (2012). Effect of transition metal oxides catalysts on oxidative desulfurization of model diesel. *Fuel processing technology*, *101*, 78-84.

Bernal, H. G., & Caero, L. C. (2005). Solvent effects during oxidation-extraction desulfurization process of aromatic sulfur compounds from fuels. *International Journal of Chemical Reactor Engineering*, *3*, 1.

Brégeault, J. M. (2003). Transition-metal complexes for liquid-phase catalytic oxidation: some aspects of industrial reactions and of emerging technologies. *Dalton Transactions*, (17), 3289-3302.

Campos-Martin, J. M., Capel-Sanchez, M. D. C., Perez-Presas, P., & Fierro, J. L. G. (2010). Oxidative processes of desulfurization of liquid fuels. *Journal of Chemical Technology & Biotechnology*, *85*(7), 879-890.

Cedeño-Caero, L., & Alvarez-Amparan, M. A. (2014). Performance of molybdenum oxide in spent hydrodesulfurization catalysts applied on the oxidative desulfurization process of dibenzothiophene compounds. *Reaction Kinetics, Mechanisms and Catalysis*, *113*(1), 115-131.

Cedeño-Caero, L., Gomez-Bernal, H., Fraustro-Cuevas, A., Guerra-Gomez, H. D., & Cuevas-Garcia, R. (2008). Oxidative desulfurization of synthetic diesel using supported catalysts: Part III. Support effect on vanadium-based catalysts. *Catalysis Today*, *133*, 244-254.

Daniel, M. F., Desbat, B., Lassegues, J. C., Gerand, B., & Figlarz, M. (1987). Infrared and Raman study of WO3 tungsten trioxides and WO3, xH2O tungsten trioxide tydrates. *Journal of solid state chemistry*, *67*(2), 235-247.

Qian, E. W. (2008). Development of Novel Nonhydrogenation Desulfurization Process -Oxidative Desulfurization of Distillate-.*Journal of the Japan Petroleum Institute,* 51, 24-31.

International Energy Outlook 2016: (2016). *With Projections to 2040*. Energy Information Administration (US), & Government Publications Office (2016). (Eds.). Government Printing Office, 1, 19-35.

Fierro, J. L. G. (2005). *Metal oxides: chemistry and applications*. CRC press,1, 18-30.

García-Gutiérrez, J. L., Fuentes, G. A., Hernández-Terán, M. E., Garcia, P., Murrieta-Guevara, F., & Jiménez-Cruz, F. (2008). Ultra-deep oxidative desulfurization of diesel fuel by the Mo/Al2O3-H2O2 system: The effect of system parameters on catalytic activity. *Applied Catalysis A: General*, *334*(1-2), 366-373.

González-García, O., & Cedeño-Caero, L. (2009). V-Mo based catalysts for oxidative desulfurization of diesel fuel. *Catalysis Today*, *148*(1-2), 42-48.

González-García, O., & Cedeño-Caero, L. (2010). V-Mo based catalysts for ods of diesel fuel. Part II. Catalytic performance and stability after redox cycles. *Catalysis Today*, *150*(3-4), 237-243.

Horsley, J. A., Wachs, I. E., Brown, J. M., Via, G. H., & Hardcastle, F. D. (1987). Structure of surface tungsten oxide species in the tungsten trioxide/alumina supported oxide system from x-ray absorption near-edge spectroscopy and Raman spectroscopy. Journal of Physical Chemistry, 91(15), 4014-4020.

Ishihara, A., Wang, D., Dumeignil, F., Amano, H., Qian, E. W., & Kabe, T. (2005). Oxidative desulfurization and denitrogenation of a light gas oil using an oxidation/adsorption continuous flow process. Applied Catalysis A: General, 279(1-2), 279-287.

Ismagilov, Z., Yashnik, S., Kerzhentsev, M., Parmon, V., Bourane, A., Al-Shahrani, F. M., ... & Koseoglu, O. R. (2011). Oxidative desulfurization of hydrocarbon fuels. Catalysis Reviews, 53(3), 199-255.

Kim, T., Burrows, A., Kiely, C. J., & Wachs, I. E. (2007). Molecular/electronic structure–surface acidity relationships of model-supported tungsten oxide catalysts. Journal of Catalysis, 246(2), 370-381.

Kuzmin, A., Purans, J., Cazzanelli, E., Vinegoni, C., & Mariotto, G. (1998). X-ray diffraction, extended x-ray absorption fine structure and Raman spectroscopy studies of WO3 powders and (1− x) WO 3− y· x ReO 2 mixtures. Journal of applied Physics, 84(10), 5515-5524.

Leofanti, G., Tozzola, G., Padovan, M., Petrini, G., Bordiga, S., & Zecchina, A. (1997). Catalyst characterization: characterization techniques. Catalysis today, 34(3-4), 307-327.

Li, X., Zhu, H., Wang, A., Wang, Y., & Chen, Y. (2012). Oxidative Desulfurization of Dibenzothiophene over Tungsten Oxides Supported on SiO_2 and γ-Al_2O_3. Chemistry letters, 42(1), 8-10.

Feng, M. (2010). Review on Recent Patents in Sulfur Removal from Liquid Fuels by Oxidative Desulfurization (ODS) Process. Recent Patents on Chemical Engineering, 3, 30-37.

Mangnus, P. J., Bos, A., & Moulijn, J. A. (1994). Temperature-programmed reduction of oxidic and sulfidic alumina-supported NiO, WO3, and NiO-WO3 catalysts. Journal of Catalysis, 146(2), 437-448.

Massoth, F. E. (1979). Characterization of molybdena catalysts. In Advances in catalysis (Vol. 27, pp. 265-310). Academic Press.

Mitra, B., Wachs, I. E., & Deo, G. (2006). Promotion of the propane ODH reaction over supported V2O5/Al2O3 catalyst with secondary surface metal oxide additives. Journal of Catalysis, 240(2), 151-159.

Mjalli, F. S., Ahmed, O. U., Al-Wahaibi, T., Al-Wahaibi, Y., & AlNashef, I. M. (2014). Deep oxidative desulfurization of liquid fuels. Reviews in Chemical Engineering,30(4),337-378.

Mokhtar, W. N. A. W., Bakar, W. A. W. A., Ali, R., & Kadir, A. A. A. (2016). Development of bimetallic and trimetallic oxides doped on molybdenum oxide based material on oxidative desulfurization of diesel. Arabian Journal of Chemistry.

Murata, S., Murata, K., Kidena, K., & Nomura, M. (2004). A novel oxidative desulfurization system for diesel fuels with molecular oxygen in the presence of cobalt catalysts and aldehydes. *Energy & Fuels*, *18*(1), 116-121.

NOM-086-SEMARNAT-SENER-SCFI-2005. (2008). *SEMARNAT-SENER-SCFI, Fossil fuel specifications for environmental protection*. 1, 1-13.

Ogata, E., Kamiya, Y., & Ohta, N. (1973). The effect of oxidation state of tungsten on hydrocracking of n-heptane over tungsten oxide. *Journal of Catalysis*, *29*(2), 296-307.

OPEC. (2011). *World Oil Outlook, Viena: Organisation of Petroleum Exporting Countries*. 1, 59-72.

Ostromecki, M. M., Burcham, L. J., & Wachs, I. E. (1998). The influence of metal oxide additives on the molecular structures of surface tungsten oxide species on alumina. II. In situ conditions. Journal of Molecular Catalysis A: Chemical, 132(1), 59-71.

Ostromecki, M. M., Burcham, L. J., Wachs, I. E., Ramani, N., & Ekerdt, J. G. (1998). The influence of metal oxide additives on the molecular structures of surface tungsten oxide species on alumina: I. Ambient conditions. *Journal of Molecular Catalysis A: Chemical*, *132*(1), 43-57.

Otsuki, S., Nonaka, T., Takashima, N., Qian, W., Ishihara, A., Imai, T., & Kabe, T. (2000). Oxidative desulfurization of light gas oil and vacuum gas oil by oxidation and solvent extraction. *Energy & fuels*, *14*(6), 1232-1239.

Rafiee, E., Sahraei, S., & Moradi, G. R. (2016). Extractive oxidative desulfurization of model oil/crude oil using KSF montmorillonite - supported 12-tungstophosphoric acid. *Petroleum Science*, *13*(4), 760-769.

Reddy, E. P., & Varma, R. S. (2004). Preparation, characterization, and activity of Al2O3-supported V2O5 catalysts. *Journal of catalysis*, *221*(1), 93-101.

Rezvani, M. A., Oveisi, M., & Asli, M. A. N. (2015). Phosphotungestovanadate immobilized on PVA as an efficient and reusable nano catalyst for oxidative desulphurization of gasoline. *Journal of Molecular Catalysis A: Chemical*, *410*, 121-132.

Salvati Jr, L., Makovsky, L. E., Stencel, J. M., Brown, F. R., & Hercules, D. M. (1981). Surface spectroscopic study of tungsten-alumina catalysts using X-ray photoelectron, ion scattering, and Raman spectroscopies. *The Journal of Physical Chemistry*, *85*(24), 3700-3707.

Schneider, P., Hudec, P., & Solcova, O. (2008). Pore-volume and surface area in microporous – mesoporous solids. *Microporous and mesoporous materials*, *115*(3), 491-496.

Song, C. (2003). An overview of new approaches to deep desulfurization for ultra-clean gasoline, diesel fuel and jet fuel. *Catalysis today*, *86*(1-4), 211-263.

Speight, J. G., & El-Gendy, N. S. (2015). *Handbook of refinery desulfurization*. CRC Press.

Stanislaus, A., Marafi, A., & Rana, M. S. (2010). Recent advances in the science and technology of ultra-low sulfur diesel (ULSD) production. *Catalysis today*, *153*(1-2), 1-68.

Te, M., Fairbridge, C., & Ring, Z. (2001).Oxidation reactivities of dibenzothiophenes in polyoxometalate/H_2O_2 and formic acid/H_2O_2 systems.*Applied Catalysis A: General*, *219*(1-2), 267-280.

Thomas, R., De Beer, V. H. J., & Moulijn, J. A. (1981). A temperature programmed reduction study of gamma-alumina supported molybdenum and tungsten oxide. *Bulletin des Societes Chimiques Belges*, *90*(12), 1349-1357.

Vermaire, D. C., & Van Berge, P. C. (1989). The preparation of WO3TiO2 and Wo3Al2O3 and characterization by temperature-programmed reduction. *Journal of catalysis*, *116*(2), 309-317.

Vuurman, M. A., & Wachs, I. E. (1992). In situ Raman spectroscopy of alumina-supported metal oxide catalysts. *The Journal of Physical Chemistry*, *96*(12), 5008-5016.

Vuurman, M. A., Stufkens, D. J., Oskam, A., Deo, G., & Wachs, I. E. (1996). Combined Raman and IR study of MO x–V 2 O 5/Al 2 O 3 (MO x= MoO 3, WO 3, NiO, CoO) catalysts under dehydrated conditions. *Journal of the Chemical Society, Faraday Transactions*, *92*(17), 3259-3265.

Wachs, I. E., & Roberts, C. A. (2010). Monitoring surface metal oxide catalytic active sites with Raman spectroscopy. Chemical Society Reviews, 39(12), 5002-5017.

Wachs, I. E., Chersich, C. C., & Iiardenbergh, J. H. (1985). Reduction of W03/A1203 and unsopported W03: A comparative ESCA study. *Applied catalysis*, *13*(2), 335-346.

Weckhuysen, B. M., Jehng, J. M., & Wachs, I. E. (2000). In situ Raman spectroscopy of supported transition metal oxide catalysts: 18O2− 16O2 Isotopic Labeling Studies. *The Journal of Physical Chemistry B*, *104*(31), 7382-7387.